DETERMINATION OF PARAMETERS FOR EVERGREEN BROADLEAF FORESTS IN GROSS PRIMARY PRODUCTION CAPACITY ESTIMATION ALGORITHM

Aika Wakai (1), Rinako Yoshioka (1), Kanako Muramatsu (1)

[1] Nara Women's University, Kita-Uoya-Nishimachi, Nara, 630-8506, Japan
Email: wakai-aika6492@es.nara-wu.ac.jp; muramatu@es.nara-wu.ac.jp

KEY WORDS: gross primary production, light-response curve of photosynthesis, chlorophyll, evergreen broadleaf forests, MODIS

ABSTRACT: An algorithm for estimating gross primary production capacity (GPPcapacity) which is gross primary production (GPP) without stresses using satellite data was developed in a previous study. This algorithm assumes the relationship between instantaneous values of photosynthetic active radiation (PAR) and GPPcapacity as nonlinear and enables us to estimate instantaneous values of GPPcapacity. The maximum values of GPPcapacity depends on chlorophyll content. Chlorophyll index (CI) calculated from satellite data is considered to have linear relationships with maximum values of GPPcapacity. Parameters in this algorithm are determined for each vegetation type in each climate region. Parameters for tropical evergreen broadleaf forests (EBF) were not determined because the linear regression had a weak correlation because of the limited range of CI and the maximum values of GPPcapacity caused by using the data without clouds in only dry season. It was considered the linear regression for EBF should be determined together with the data for EBF in other climate zone like temperate zone.

In this study, ground-observed flux data and satellite data of MODIS for a temperate EBF site in Australia were newly analyzed to determine parameters for EBF using the Australian data and the data for tropical sites in Amazon and Thailand. The values of CI and the maximum rate of photosynthesis for the Australian site were smaller than both Amazonian and Thailand sites. CI and the maximum rate of photosynthesis had a strong linear correlation with R=0.80 when the data for all the sites were fitted together, parameters common for EBF were determined. GPPcapacity was estimated using determined parameters and MODIS data every 30 minutes for the Australian site, and 1 hour for one of the Amazonian site. We examined whether GPPcapacity could be regarded as a first approximation of GPP and whether GPPcapacity could be estimated using parameters common for EBF. Moreover, the relationship between PAR and the ratio of GPP to GPPcapacity was examined.

The ratio of GPP to GPPcapacity from flux data ($GPPcap_{flux}$) was 1.00 ± 0.02 for Australian and 1.01 ± 0.01 for Amazonian site. Hence, GPPcapacity could be regarded as a first approximation of GPP for both sites. The ratio of $GPPcap_{flux}$ to GPPcapacity estimated using determined parameters and MODIS data ($GPPcap_{MODIS}$) was 0.930 ± 0.004 for Australian and 1.014 ± 0.008 for Amazonian site. $GPPcap_{MODIS}$ was overestimated for Australian site, on the other hand, it was a little underestimated for Amazonian site. From the results of comparing $GPPcap_{MODIS}$ to GPP, GPP was 0.92 times $GPPcap_{MODIS}$ for Australian site, and GPP was almost same as $GPPcap_{MODIS}$ for Amazonian site. The relationship between PAR and the ratio of GPP to both $GPPcap_{flux}$ and $GPPcap_{MODIS}$ had a same tendency for the two sites. The ratio became close to 1.0 rapidly when PAR < 200 $\mu molm^{-2}s^{-1}$ for Australian site and PAR < 100 $\mu molm^{-2}s^{-1}$ for Amazonian site, and then gradually became to be constant as PAR increased. Therefore, we can calculate GPP accurately at higher PAR values by estimating $GPPcap_{MODIS}$ instead for both sites.

1. INTRODUCTION

The concentration of CO_2 is the highest among the greenhouse gases and terrestrial ecosystem sequesters 20 to 30 % of anthropogenic CO_2 (Saleska *et al*., 2003). Improving the estimation accuracy of gross primary production (GPP) which is the amount of CO_2 absorbed by plants via photosynthesis contributes to reveal carbon cycle. Especially, it is important to estimate GPP in evergreen broadleaf forests (EBF) because they occupy about 20% of global forest area (Schmitt *et al*., 2009).

Light-use efficiency (LUE) model (Monteith, 1972) is widely used to estimate GPP using satellite data. LUE model assumes a linear relationship between accumulated values of photosynthetically active radiation (PAR) and GPP in a certain period such as a month or a year. On the other hand, their instantaneous relationship is nonlinear.

The rate of photosynthesis relates photosynthetic capacity and photosynthesis reduction caused by weather conditions. Thanyapraneedkul *et al*. (2012) defines gross primary production capacity (GPPcapacity) as GPP without environmental stresses focusing on photosynthetic capacity and develops GPPcapacity estimation algorithm to

estimate it using satellite data. The relationship between instantaneous PAR and GPPcapacity values are determined using light-response curves of photosynthesis. Maximum values of GPPcapacity in the light-response curves of photosynthesis are related to chlorophyll content. Chlorophyll index (CI) is calculated using satellite data, and then GPPcapacity is estimated. This algorithm enables us to estimate instantaneous GPPcapacity values using instantaneous PAR values.

Parameters in the light-response curve of photosynthesis are determined using ground-observed PAR and GPPcapacity values. The relationship between CI and maximum GPPcapacity values are considered to be linear. Parameters in the linear regressions are determined using satellite-observed CI and ground-observed GPPcapacity for each vegetation type in each climate region. In previous studies, parameters for grass, paddy, shrubs, deciduous needleleaf forests, deciduous broadleaf forests and evergreen needleleaf forests were determined (Thanyapraneedkul *et al*., 2012; Mineshita *et al*., 2016: Muramatsu *et al*., 2017). However, parameters for EBF has not been determined yet because of the limited availability of the data in dry season for only one tropical EBF site in Thailand (TH-SKR) (Thanyapraneedkul *et al*., 2012).

Parameters for tropical EBF in Amazon were tried to be determined for the importance of estimating GPPcapacity in Amazon (Doughty *et al*., 2008). Satellite data of an optical sensor for Amazon were affected by clouds in rainy season. The data only in dry season had limited range of CI and GPPcapacity causing a low correlation between them. Moreover, the data for TH-SKR (Thanyapraneedkul *et al*., 2012) showed the similar low correlation. From these results, we considered that it was difficult to determine the parameters with the data for EBF only in the tropical zone, and the data in other climate zones such as the temperate zone should be studied together.

The objectives of this study are to determine parameters in the linear regression common for EBF in Australia, Amazon and Thailand and to estimate GPPcapacity for an Australian and an Amazonian site using them. To achieve these objectives, the data for temperate EBF in Australia was newly analyzed in this study. It was also examined whether estimated GPPcapacity was regarded as a first approximation of GPP.

2. DATA

We used flux data for an Australian and two Amazonian sites as ground-observed data. MODIS data corresponding to flux sites were used as satellite data.

2.1 Flux Data

Flux data for Whroo site (AU-Whr) in Australia, Santarem-Km67-Primary Forest site (BR-Sa1) and Santarem-Km83-Logged Forest site (BR-Sa3) in Amazon were downloaded from FLUXNET2015 Dataset site (FLUXNET2015). AU-Whr locates at 36.6732°S, 145.0294°E where climate is humid subtropical. BR-Sa1 and BR-Sa3 locates at 2.8567° S, 54.9589°W and 3.0180°S, 54.9714°W where climate is tropical monsoon. All the sites had homogeneous vegetation of EBF more than 2 square kilometers when the data were acquired. The data acquired from August 29, 2013 to December 31, 2014 were used for AU-Whr, between 2002 and 2004 and between 2009 and 2011 for BR-Sa1, from June 25, 2000 to March 12, 2004 for BR-Sa3. PAR, daytime-based GPP and vapor pressure deficit (VPD) data were used. PAR data for AU-Whr were provided by the principal investigator of AU-Whr. When flux data did not have these data or had abnormal values of them, they were not used. The time periods of the data were 30 minutes for AU-Whr and BR-Sa3, and 1 hour for BR-Sa1. Used data versions were version 2-3 for AU-Whr, and 1-3 for BR-Sa1 and BR-Sa3.

2.2 MODIS Data

MODIS surface reflectance data (MOD09A1) were downloaded from ORNL DAAC site (ORNL DAAC, 2017; ORNL DAAC, 2018; Vermote, 2015). The data for one pixel corresponding to the coordinates of each flux site were used. Data period was 8 days and their spatial resolution was 500 m. Used data version was collection 6.

3. METHODS

3.1 Data Preprocessing

3.1.1 Selecting GPPcapacity Data from GPP Data: GPP data without stress of dryness were selected as GPPcapacity data using the same methods as Thanyapraneedkul *et al.* (2012). When GPP values decrease though PAR values increase during daytime, plants have stress of dryness. VPD values at the time when GPP began to decrease were examined and 1.5 kPa was determined as VPD threshold for all sites. GPP data with VPD values less

than 1.5 kPa were selected as GPPcapacity data.

3.1.2 Selecting MODIS Data without Clouds for Amazonian Sites: MODIS data for Amazonian sites (BR-Sa1 and BR-Sa3) were considered to be affected by clouds in rainy season. MODIS data without clouds were selected by setting conditions of MODIS quality assurance cloud flags (Vermote *et al*., 2015) and spectral reflectance values. The data with cloud flags of "cloud state was clear, mixed or not set/assumed clear", "cloud shadow did not exist", "aerosol quantity was low" and "cirrus was not detected, small or average amount of it was detected" were selected. Then, the data when reflectance values of both blue (Blue) and red (Red) bands were lower than 0.1and green (Green) band was higher than Blue and Red were selected. Almost all the selected data under these conditions were acquired in dry season.

3.2 Determination of Parameters in the Light-Response Curve of Photosynthesis

Instantaneous values of PAR and GPPcapacity have non-linear relationships as shown in Fig. 1. GPPcapacity is written as a function of PAR as

$$\mathrm{GPPcapacity(PAR)} = \frac{\mathrm{GPPcap_{max}} \times slope \times \mathrm{PAR}}{1 + slope \times \mathrm{PAR}}, \tag{1}$$

where $\mathrm{GPPcap_{max}}$ is maximum value of GPP related to the chlorophyll content and slope is initial slope in the light-response curve of photosynthesis (Thanyapraneedkul *et al*., 2012). Eq. 1 was fitted to the flux data of PAR and GPPcapacity every 8-day period corresponding to the data period of MODIS. $\mathrm{GPPcap_{max}}$ values were determined for every 8-day period. On the other hand, *slope* values determined for every 8-day period were averaged for each year, and then they were averaged for all years. Therefore, each site has one *slope* value. In the case of Amazonian sites, two *slope* values specific to BR-Sa1 and BR-Sa3 were averaged and they had one common *slope* value.

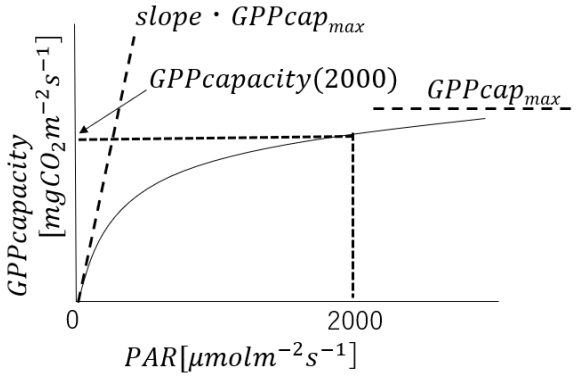

Figure 1. Light-Response Curve of Photosynthesis. $\mathrm{GPPcap_{max}}$ and *slope* are Parameters. $\mathrm{GPPcap_{max}}$ is Maximum GPPcapacity and *slope* Relates to the Initial Slope. GPPcapacity(2000) is GPPcapacity when PAR is 2000 $\mu molm^{-2}s^{-1}$.

3.3 The Ratio of GPP to GPPcapacity from Flux Data

The ratio of GPP to GPPcapacity from flux data ($\mathrm{GPPcap_{flux}}$) was calculated to verify whether $\mathrm{GPPcap_{flux}}$ was regarded as a first approximation of GPP. $\mathrm{GPPcap_{flux}}$ was calculated using Eq. 1 with determined parameters every 30 minutes for AU-Whr, and 1 hour for BR-Sa1, respectively. The data when PAR values were higher than 1.0 $\mu molm^{-2}s^{-1}$ were used to select the data in daytime without measurement noises of the sensor. The weighted mean of the ratio of GPP to $\mathrm{GPPcap_{flux}}$ and its standard deviation were calculated with the data in all years as

$$\frac{\overline{\mathrm{GPP}}}{\mathrm{GPPcap_{flux}}} = \frac{\sum_{i=1}^{n}\left(\mathrm{GPP_i} \times \left(\frac{\mathrm{GPP}}{\mathrm{GPPcap_{flux}}}\right)_i\right)}{\sum_{i=1}^{n}\mathrm{GPP_i}}, (i = 1, \cdots, n) \tag{2}$$

and

$$\sigma = \sqrt{\frac{\sum_{i=1}^{n}\left(\mathrm{GPP_i} \times \left(\mathrm{GPP_i} - \frac{\overline{\mathrm{GPP}}}{\mathrm{GPPcap_{flux}}}\right)^2\right)}{(n-1)\sum_{i=1}^{n}\mathrm{GPP_i}}}. (i = 1, \cdots, n) \tag{3}$$

Moreover, the relationship between PAR and $\left|\frac{\mathrm{GPP}}{\mathrm{GPPcap_{flux_i}}}-1\right|$ was examined to make it clear that how much differences there are between $\mathrm{GPPcap_{flux}}$ and GPP depending on PAR values.

3.4 The Relationship between CI and GPPcapacity(2000) Common for EBF in Australia, Amazon and Thailand

CI was calculated every 8-day period using MODIS reflectance data of Green and near infrared band (NIR) as

$$\mathrm{CI}=\frac{\mathrm{NIR}}{\mathrm{Green}}-1, \tag{4}$$

(Gitelson *et al*., 2003). GPPcapacity(2000) values (i.e. the value of GPPcapacity where PAR is enough high value of 2000 $\mu\mathrm{molm^{-2}s^{-1}}$) were calculated every 8-day period by substituting parameters in the light-response curve of photosynthesis into Eq. 1. A linear regression

$$\mathrm{GPPcapacity}(2000)=\mathrm{a}\times\mathrm{CI}+\mathrm{b}, \tag{5}$$

was fitted to the data of CI and GPPcapacity(2000) for AU-Whr, BR-Sa1, BR-Sa3 and TH-SKR (Thanyapraneedkul *et al*., 2012) at once and parameters in Eq. 5 (a and b) were determined as common parameters for EBF.

3.5 GPPcapacity Estimation Using CI and Determined Parameters

GPPcapacity values were estimated using CI, parameters in the linear regression common for EBF and *slope* in the light-response curve of photosynthesis ($\mathrm{GPPcap_{MODIS}}$) for AU-Whr and BR-Sa1. First, $\mathrm{GPPcap_{max}}$ was estimated as

$$\mathrm{GPPcap_{max}}=\frac{\mathrm{GPPcapacity}(2000)\times(1+slope\times 2000)}{slope\times 2000}. \tag{6}$$

Then, $\mathrm{GPPcap_{MODIS}}$ values were estimated every 30 minutes for AU-Whr and 1 hour for BR-Sa1when PAR values were higher than 1.0 $\mu\mathrm{molm^{-2}s^{-1}}$ with Eq. 1 by substituting Eq. 6 into it.

The ratio of $\mathrm{GPPcap_{flux}}$ to $\mathrm{GPPcap_{MODIS}}$ was calculated to examine whether $\mathrm{GPPcap_{MODIS}}$ could be estimated using parameters in the linear regression common for EBF. Weighted mean and standard deviation were calculated for each site as

$$\overline{\frac{\mathrm{GPPcap_{flux}}}{\mathrm{GPPcap_{MODIS}}}}=\frac{\sum_{\mathrm{i=1}}^{\mathrm{n}}\left(\mathrm{GPPcap_{flux_i}}\times\left(\frac{\mathrm{GPPcap_{flux}}}{\mathrm{GPPcap_{MODIS}}}\right)_{\mathrm{i}}\right)}{\sum_{\mathrm{i=1}}^{\mathrm{n}}\mathrm{GPPcap_{flux_i}}},(\mathrm{i}=1,\cdots,\mathrm{n}) \tag{7}$$

and

$$\sigma=\sqrt{\frac{\sum_{\mathrm{i=1}}^{\mathrm{n}}\left(\mathrm{GPPcap_{flux_i}}\times\left(\mathrm{GPPcap_{flux_i}}-\overline{\frac{\mathrm{GPPcap_{flux}}}{\mathrm{GPPcap_{MODIS}}}}\right)^{2}\right)}{(\mathrm{n}-1)\sum_{\mathrm{i=1}}^{\mathrm{n}}\mathrm{GPPcap_{flux_i}}}}.(\mathrm{i}=1,\cdots,\mathrm{n}) \tag{8}$$

Moreover, the ratio of GPP to $\mathrm{GPPcap_{MODIS}}$ was calculated to make an equation for estimating GPP from $\mathrm{GPPcap_{MODIS}}$. Weighted mean and standard deviation of the ratio were calculated for each site as

$$\overline{\frac{\mathrm{GPP}}{\mathrm{GPPcap_{MODIS}}}}=\frac{\sum_{\mathrm{i=1}}^{\mathrm{n}}\left(\mathrm{GPP_i}\times\left(\frac{\mathrm{GPP}}{\mathrm{GPPcap_{MODIS}}}\right)_{\mathrm{i}}\right)}{\sum_{\mathrm{i=1}}^{\mathrm{n}}\mathrm{GPP_i}},(\mathrm{i}=1,\cdots,\mathrm{n}) \tag{9}$$

and

$$\sigma = \sqrt{\frac{\sum_{i=1}^{n}\left(GPP_i \times \left(GPP_i - \overline{\frac{GPP}{GPPcap_{MODIS}}}\right)^2\right)}{(n-1)\sum_{i=1}^{n} GPP_i}}. (i = 1, \cdots, n) \quad (10)$$

The ratio of $GPPcap_{flux}$ to $GPPcap_{MODIS}$ and GPP to $GPPcap_{MODIS}$ were calculated every 30 minutes for AU-Whr, and 1 hour for BR-Sa1.

The relationship between PAR and $\left|\frac{GPP}{GPPcap_{MODIS_i}} - 1\right|$ was examined for each site to examine how $GPPcap_{MODIS}$ values were different from GPP values depending on PAR values.

4. RESULTS

4.1 Parameters in the Light-Response Curve of Photosynthesis

slope value for AU-Whr was 0.00152±0.00001, common for BR-Sa1 and BR-Sa3 was 0.0013±0.0001.

4.2 The Ratio of GPP to GPPcapacity from Flux Data

$\overline{\frac{GPP}{GPPcap_{flux}}}$ for AU-Whr was 1.00±0.02, and for BR-Sa1 was 1.01±0.01. Hence, GPPcapacity could be regarded as a first approximation of GPP for both AU-Whr and BR-Sa1.

Fig. 2 shows the relationship between PAR and $\left|\frac{GPP}{GPPcap_{flux_i}} - 1\right|$ for AU-Whr (Fig. 2 (a)) and for BR-Sa1 (Fig. 2 (b)). According to Fig. 2 (a), for AU-Whr, when PAR < 200 μmolm^{-2}s^{-1}, the higher PAR values were, the values of $\left|\frac{GPP}{GPPcap_{flux}} - 1\right|$ rapidly decreased. When PAR ≥ 200 μmolm^{-2}s^{-1}, most of them were less than 0.4 and the range of them gradually became to be constant. According to Fig. 2 (b), for BR-Sa1, when PAR < 100 μmolm^{-2}s^{-1}, the values of $\left|\frac{GPP}{GPPcap_{flux}} - 1\right|$ were rapidly decreased. When PAR ≥ 100 μmolm^{-2}s^{-1}, most of them were less than 0.2 and distributed close to 0. Their range became to be constant at a lower PAR value than AU-Whr.

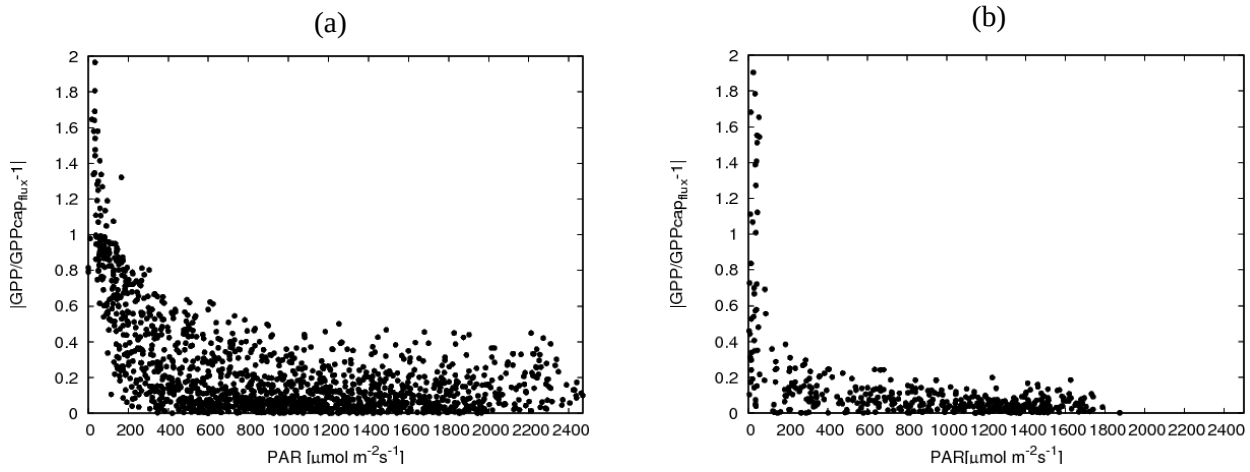

Figure 2. The Relationship between PAR and $\left|\frac{GPP}{GPPcap_{flux}} - 1\right|$ when PAR > 1.0 μmolm^{-2}s^{-1} for (a) AU-Whr and (b) BR-Sa1 with $\left|\frac{GPP}{GPPcap_{flux}} - 1\right| \leq 2.0$.

4.3 The Relationship between CI and GPPcapacity(2000) Common for EBF in Australia, Amazon and Thailand

Fig. 3 shows the relationship between CI and GPPcapacity(2000) for EBF in Australia, Amazon and Thailand. Most of CI values for Amazonian and Thailand sites were around 8. On the other hand, those for Australia were between 2 and 7. The linear regression common for them was determined as

$$\mathrm{GPPcapacity}(2000) = 0.121 \times \mathrm{CI} + 0.16, \quad (11)$$

with R=0.80.

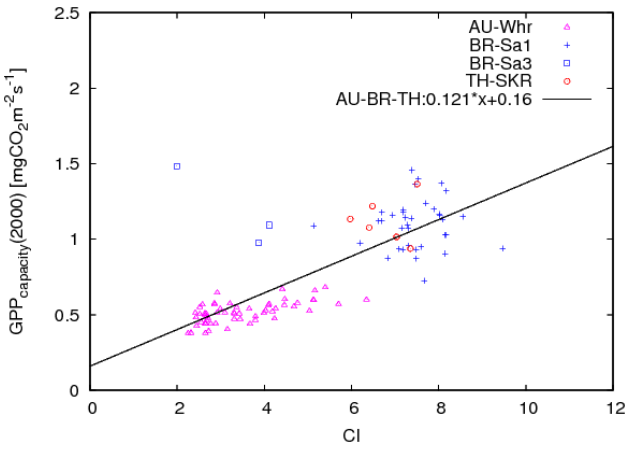

Figure 3. The Relationship between CI and GPPcapacity(2000) for EBF in Australia, Amazon and Thailand. Pink Triangles, Blue Crosses, Blue Squares and Red Circles are the Data for AU-Whr, BR-Sa1, BR-Sa3 and TH-SKR (Thanyapraneedkul *et al.*, 2012), Respectively. Black Line of 0.121x+0.16 is the Linear Regression Common for Them with R=0.80.

4.4 GPPcapacity Estimated Using CI and Determined Parameters

$\overline{\frac{\mathrm{GPPcap_{flux}}}{\mathrm{GPPcap_{MODIS}}}}$ was 0.930±0.004 for AU-Whr, and 1.014±0.008 for BR-Sa1. For AU-Whr, $\mathrm{GPPcap_{MODIS}}$ was overestimated. On the other hand, for BR-Sa1, it was a little underestimated.

$\overline{\frac{\mathrm{GPP}}{\mathrm{GPPcap_{MODIS}}}}$was 0.92±0.02 for AU-Whr, and 1.02±0.02 for BR-Sa1. Fig. 4 shows the relationship between PAR and $\left|\frac{\mathrm{GPP}}{\mathrm{GPPcap_{MODIS_i}}} - 1\right|$ for AU-Whr (Fig. 4 (a)) and BR-Sa1 (Fig. 4 (b)). It had almost the same tendency as the relationship between PAR and $\left|\frac{\mathrm{GPP}}{\mathrm{GPPcap_{flux}}} - 1\right|$ as shown in Fig. 2. However, the range of $\left|\frac{\mathrm{GPP}}{\mathrm{GPPcap_{MODIS}}} - 1\right|$was larger than $\left|\frac{\mathrm{GPP}}{\mathrm{GPPcap_{flux}}} - 1\right|$ when they became to be constant, especially for BR-Sa1.

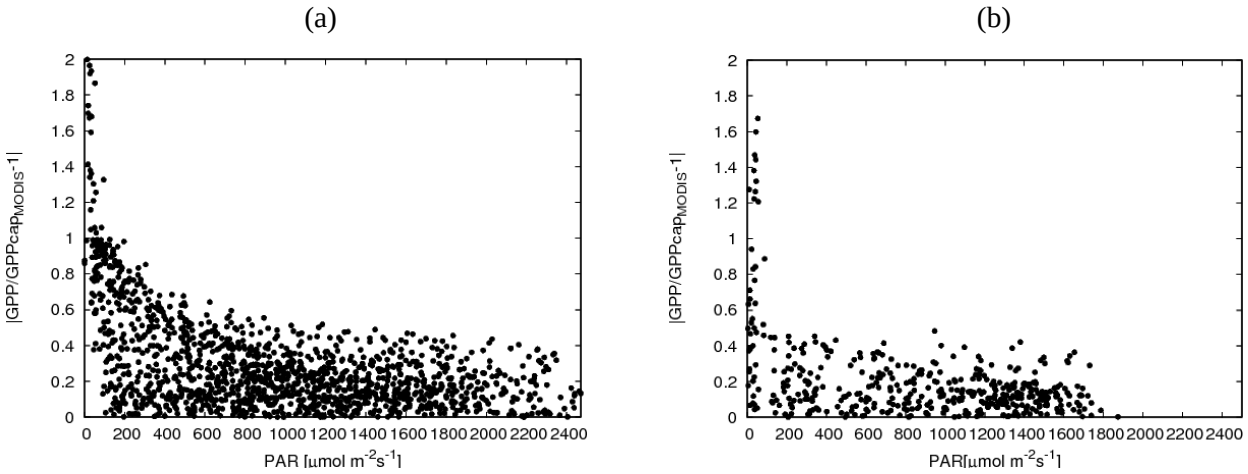

Figure 4. The Relationship between PAR and $\left|\frac{\mathrm{GPP}}{\mathrm{GPPcap_{MODIS}}} - 1\right|$ for (a) AU-Whr and (b) BR-Sa1 with $\left|\frac{\mathrm{GPP}}{\mathrm{GPPcap_{MODIS}}} - 1\right| \leq 2.0$.

5. DISCUSSION and CONCLUSIONS

5.1 The Ratio of GPP to GPPcapacity from Flux Data

The ratio of GPP to $GPPcap_{flux}$ was calculated every 30 minutes for AU-Whr and 1 hour for BR-Sa1 using determined parameters in the light-response curve of photosynthesis and PAR values. When PAR values were higher than 1.0 $\mu molm^{-2}s^{-1}$, the average ratio of GPP to $GPPcap_{flux}$ was 1.00 ± 0.02 for AU-Whr, and 1.01 ± 0.01 for BR-Sa1. Hence, $GPPcap_{flux}$ was regarded as a first approximation of GPP for both sites. As PAR values became higher, its standard deviation rapidly decreased initially, and then gradually became to be constant (Fig. 2). It means $GPPcap_{flux}$ values tend to be closer to GPP at higher PAR values.

5.2 The Relationship between CI and GPPcapacity(2000)

The linear regression common for EBF in Australia, Amazon and Thailand was determined. The values of CI and GPPcapacity(2000) for Amazon were almost same as Thailand site (Thanyapraneedkul *et al*., 2012), but larger than Australia. The range of CI for AU-Whr was wider than Amazon and Thailand (Thanyapraneedkul *et al*., 2012) because the data for Amazon and Thailand (Thanyapraneedkul *et al*., 2012) were without clouds and they were acquired in dry season, the range of CI was smaller than Australia which has the data acquired in all seasons. Parameters in the linear regression common for EBF was determined because of the differences of their different ranges and values.

5.3 GPPcapacity Estimated Using CI and Determined Parameters

$GPPcap_{MODIS}$ values were estimated using CI, determined parameters and PAR values, and the average ratio of $GPPcap_{flux}$ to $GPPcap_{MODIS}$ and GPP to $GPPcap_{MODIS}$ were calculated every 30 minutes for AU-Whr and 1 hour for BR-Sa1. The average ratio of $GPPcap_{flux}$ to $GPPcap_{MODIS}$ was 0.930 ± 0.004 for AU-Whr and 1.014 ± 0.008 for BR-Sa1. $GPPcap_{flux}$ was overestimated for AU-Whr, on the other hand, a little underestimated for BR-Sa1 using common parameters for EBF. The average ratio of GPP to $GPPcap_{MODIS}$ was 0.92 ± 0.02 for AU-Whr and 1.02 ± 0.02 for BR-Sa1. For AU-Whr, GPP could be estimated by estimating $GPPcap_{MODIS}$ values as

$$\mathrm{GPP} = 0.92 \times \mathrm{GPPcap}_{\mathrm{MODIS}}. \tag{12}$$

For BR-Sa1, GPP could be estimated by calculating $GPPcap_{MODIS}$ instead. For both sites, it is considered that GPP could be estimated with less standard deviation at higher PAR values because $GPPcap_{MODIS}$ tends to be closer to GPP as PAR values became higher (Fig. 4).

6. ACKNOWLEDGEMENTS

This work was supported by JSPS KAKENHI (Grant Number 16K00514). The flux data of AU-Whr, BR-Sa1 and BR-Sa3 were downloaded from FLUXNET2015 Dataset. PAR data for AU-Whr were provided by the principal investigator of AU-Whr, Jason Beringer.

7. REFERENCES

Doughty, C. E. *et al*., 2008. Are tropical forests near a high temperature threshold? Journal of Geophysical Research, 113, G00B07.

FLUXNET2015. Retrieved May 7, 2019 for AU-Whr, and June 19, 2018 for BR-Sa1 and June 2, 2017 for BR-Sa3, from http://fluxnet.fluxdata.org/data/fluxnet2015-dataset/.

Gitelson, A. A. *et al*., 2003. Relationships between leaf chlorophyll content and spectral reflectance and algorithms for non-destructive chlorophyll assessment in higher plant leaves. Journal of Plant Physiology, 160, pp. 271-282.

Mineshita, Y. *et al*., 2016. Determination of parameters for shrubs in the global gross primary production capacity estimation algorithm. Journal of the Remote Sensing Society of Japan, 36 (3), pp. 236-246.

Monteith, J. L., 1972. Solar radiation and productivity in tropical ecosystems. Journal of Applied Ecology, 9, pp. 747-766.

Muramatsu, K. *et al*., 2017. Determination of rice paddy parameters in the global gross primary production capacity estimation algorithm using 6 years of JP-MSE flux observation data. Journal of Agricultural Meteorology, 73 (3), pp. 119-132.

ORNL DAAC, 2017. MODIS Collection 6 Fixed Sites Subsetting and Visualization Tool. ORNL DAAC, Oak Ridge, Tennessee, USA, Subset Obtained for MOD09A1 Product at Site Id

'br_para_santarem_km67_primary_forest', Retrieved June 21, 2018, and 'br_para_santarem_km83_logged_forest', Retrieved July 19, 2017, from https://doi.org/10.3334/ORNLDAAC/1567.
ORNL DAAC, 2018. MODIS and VIRS Land Products Global Subsetting and Visualization Tool. ORNL DAAC, Oak Ridge, Tennessee, USA, Retrieved June 10, 2019, Subset Obtained for MOD09A1 Product at 36.6732S, 145.0294E, time period: 2000-0218 to 2019-0517, and subset size: 2.5 × 2.5 km, Retrieved May 7, 2019, from https://doi.org/10.3334/ORNLDAAC/1379.
Saleska, S. R. *et al*., 2003. Carbon in Amazon forests: Unexpected seasonal fluxes and disturbance-induced losses. Science, 302 (5650), pp. 1554-1557.
Schmitt, C. B. *et al*., 2009. Global analysis of the protection status of the world's forests. Biological Conservation, 142, pp. 2122-2130.
Thanyapraneedkul, J. *et al*., 2012. A vegetation index to estimate terrestrial gross primary production capacity for the global change observation mission-climate (GCOM-C)/second-generation global imager (SGLI) satellite sensor. Remote Sensing, 4, pp. 3689-3720.
Vermote, E. F., 2015. MOD09A1 MODIS/Terra Surface Reflectance 8-Day L3 Global 500m SIN Grid V006. NASA EOSDIS Land Processes DAAC, Retrieved May 7, 2019, from https://doi.org/10.5067/MODIS/MOD09A1.006.
Vermote, E. F. *et al*., 2015. MODIS surface reflectance user's guide Collection 6. MODIS Land Surface Reflectance Science Computing Facility.